Modelling of Temperature Distribution in Orthogonal Machining using Finite Element Method

Sunday Joshua OJOLO [a], Ahmed Amok YINUSA[a] and
Sikiru Oluwarotimi ISMAIL [b, 1]
[a] *Mechanical Engineering Department, University of Lagos, Lagos, Nigeria*
[b] *Mechanical Engineering Department, University of Portsmouth, England, UK*

Abstract. This work employs finite element method (FEM) to model the temperature distribution of a mild steel with a carbide cutting tool insert in an orthogonal machining. The finite element model was simulated with MATLAB^{TM} and validated with experimental data. The temperature rise on the shear plane and the effect of different cutting parameters such as rake angles, cutting speed and forces were investigated. The results obtained were contour and surface plots at a bottom surface z = 0 and surface z = 0.02. It shows that the minimum and maximum temperatures of 200 and 400 K were recorded at the extreme end and tip of the tool respectively, due to high friction on the tip contact area, at the bottom surface z = 0. The minimum and maximum temperatures of 285 and 310 K at the extreme end and tip of the tool were recorded respectively, at a surface z = 0.02. In addition, it was observed that an increase in temperature caused an increase in cutting speed at different rake angles. Similarly, an increased in shear force caused an increase in temperature at different rake angles. The effect of thickness on temperature rise showed that the thinner the chip, the higher the temperature on the shear plane. It was evident that the maximum temperature occurred at the tool tip, as the temperature decreased with distance away from the tool tip. Consequently, the minimum temperature occurred at the extreme end of the tool.

Keywords. Orthogonal machining, carbide tool, finite element method, variable separable, temperature distribution.

1. Introduction

During a machining process, a substantial part of the energy is converted into heat through the friction generated between the tool and workpiece, and the plastic deformation of the work material in the machining zone. Heat is generated at the primary and secondary deformation zones, but the temperature becomes maximum at the tool/chip interface [1-4]. The total heat generation due to plastic deformation and frictional sliding in the secondary deformation zone, for continuous chips produced from a non-abrasive material at medium cutting speed, can be assumed to be between 20 and 35 % of the heat generated in the primary zone [5]. The models developed by [6] and [7] provided a relatively straightforward solution for the prediction of the average temperature of the shear plane and the tool-chip interface.

Analytical model has been used to obtain the average temperature at the tool-chip interface [8], while [9] developed two similar temperature models using Wiener's energy partition analysis. A 3-D iterative model has been proposed for the distribution of the average tool-chip interface temperature in free oblique cutting based on Jaeger's friction slider solution [10]. Despite numerous research on temperature distribution in an orthogonal machining, there is no report of an outstanding model that describes the temperature distribution using finite element method as well as the method of separation of variables.

[1] Corresponding Author, S. O. Ismail, Mechanical and Design Engineering Department, University of Portsmouth, PO1 3DJ, England, United Kingdom; E-mail: sikiru.ismail@port.ac.uk

Hence, this work employs finite element method (FEM) to model the temperature distribution of a mild steel workpiece with a carbide cutting tool in an orthogonal machining. This project seeks to fulfil the following objectives: to model the temperature distribution in orthogonal machining using the FEM, to simulate the finite element model with the MATLAB^{TM} software, and to validate the model with existing data.

2. Model formulation

2.1. The model

A simplified model of the orthogonal machining process under consideration is shown in Figure 1(a). In all the models, a multi-dimensional concept was assumed. By choosing each element of the tool as a control volume, as shown in Figure 1(b).

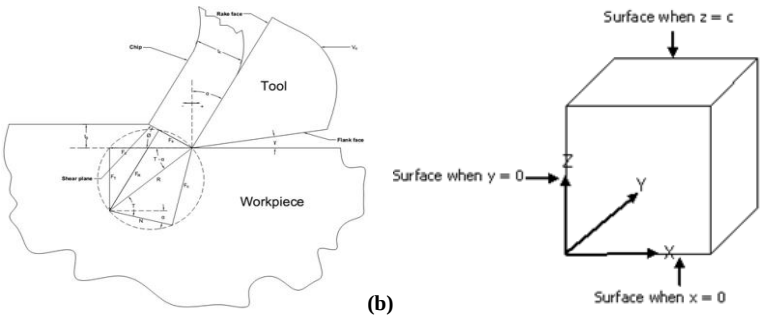

(a) **(b)**

Figure 1. (a) Simplified model of an orthogonal machining process and (b) element of the discretized model using finite element method

From the first law of thermodynamics:

$$E_{in} - E_{out} + E_{gen} = E_{stored} \quad (1)$$

The rate of heat conduction to the control volume with the dimensions of *dx, dy* and *dz* from *x, y* and *z* directions, is defined as:

$$q_x = -kdydz\frac{\partial T}{\partial x},\ q_y = -kdxdz\frac{\partial T}{\partial y},\ and\ \ q_z = -kdxdy,$$

The three dimensional heat conduction equation is; $\frac{\partial^2 T}{\partial x^2} + \frac{\partial^2 T}{\partial y^2} + \frac{\partial^2 T}{\partial z^2} = \frac{1}{\alpha_T}\frac{\partial T}{\partial t}$ (2)

Where α_T is the thermal diffusivity of the material.

2.2 Model with heat pipe

$$\frac{\partial^2 T}{\partial x^2} + \frac{\partial^2 T}{\partial y^2} + \frac{\partial^2 T}{\partial z^2} = \frac{1}{\propto}\frac{\partial T}{\partial t} \ \text{ and } \ \boldsymbol{T(x,y,z,t) = \theta + T_\infty} \quad (3)$$

Transformed equations with boundary conditions gives:

$$\left(\frac{\partial^2 \theta_1}{\partial x^2} + \frac{\partial^2 \theta_1}{\partial y^2} + \frac{\partial^2 \theta_1}{\partial z^2}\right) = \frac{1}{\propto}\frac{\partial \theta_1}{\partial t} \quad \text{and} \quad \left(\frac{\partial^2 \theta_2}{\partial x^2} + \frac{\partial^2 \theta_2}{\partial y^2} + \frac{\partial^2 \theta_2}{\partial z^2}\right) = 0 \quad (4)$$

$$\theta_1(x,y,z,t) \rightarrow transient\ state\ solution\ and\ \theta_2(x,y,z) \rightarrow steady\ state\ solution$$

Using method of separation of variables to solve the differential equations,

Thus: $\theta_2 = \sum_{m=1}^{M}\sum_{n=1}^{N} C_{mn}\left[\cos(\varepsilon_m x)\cos(\gamma_n y)\frac{\cosh(\beta z - \beta c)}{\sinh(\beta c)}\right]$ (5)

$$\boldsymbol{T(x,y,z,t) = \sum_{m=1}^{M}\sum_{n=1}^{N} T_\infty + \cos(\varepsilon_m x)\cos(\varepsilon_n y)\left[\sum_{p=1}^{\infty} C_{mnp}\cos(\varepsilon_p z)e^{-\alpha\lambda^2 t} + C_{mn}\frac{\cosh(\beta z - \beta c)}{\sinh(\beta c)}\right]} \quad (6)$$

$$\boldsymbol{T(x,y,z) = \sum_{m=1}^{M}\sum_{n=1}^{N} C_{mn}\cos(\varepsilon_m x)\cos(\varepsilon_n y)\left[\frac{\cosh(\beta z - \beta c)}{\sinh(\beta c)}\right] + T_\infty} \quad (7)$$

2.3 Model with friction

From the equation: $\frac{1}{W}\left(\frac{\partial^2 W}{\partial x^2}+\frac{\partial^2 W}{\partial y^2}\right)=-\frac{1}{B}\frac{\partial^2 B}{\partial z^2}=constant=-\beta^2$ (8)

$\frac{1}{W}\left(\frac{\partial^2 W}{\partial x^2}+\frac{\partial^2 W}{\partial y^2}\right)=-\beta^2$ and $\frac{1}{B}\frac{\partial^2 B}{\partial z^2}=\beta^2$ (9)

β is an arbitrary constant, and let $W(x,,y)=U(x)V(y)$

Hence, $\boldsymbol{\theta_2=\sum\sum A_{mn}\left[\cos(\varepsilon x)+\frac{h_1}{K\varepsilon}\sin(\varepsilon x)\right]\left[\cos(\gamma y)+\frac{\gamma h_3}{K\gamma}\sin(\gamma y)\right]}$

$\boldsymbol{[\sinh(\beta z)-N_B\cosh(\beta z)]}$ (10)

2.4 Model for heat generation

$q_c=\rho_w t_c C_w(\Delta\theta)\ and\ \Delta\theta=\frac{\lambda F_s\cos\alpha}{J\rho_w C_w\cos(\emptyset-\alpha)bt}$ [4] (11)

$q_c\ is\ dependent\ on\ friction, which\ depends\ on\ speed, depth\ of\ cut, rake\ angle.$

$Where\ \rho_w=density, C_w=specific\ heat, J=heat\ equivalent\ of\ mech.energy$

$\lambda=fraction\ of\ heat\ absorbed\ by\ chip, t_c=chip\ thickness,$

Therefore $\lambda=\frac{V\cos\alpha t\csc\emptyset\sin\emptyset}{V\cos\alpha t\csc\emptyset\sin\emptyset+2.66\varepsilon_s(\sin\emptyset\cos(\emptyset-\alpha))+A\varepsilon_s\cos\alpha}$ and $\emptyset=\tan^{-1}\left[\frac{r\cos\alpha}{1-r\sin\alpha}\right]$ (12)

$Where\ r=chip\ thickness\ ratio, \alpha=rake\ angle, V=cutting\ velocity,$

$F_s=\frac{tbk}{\sin\emptyset}, Where\ b\ and\ t=width\ \&\ depth\ of\ cut, k=yield\ stress\ of\ workpiece.$

3. Results and discussions (simulation and validation)

The parameters used to model the tool insert is shown in the Table 1.

Case 1: Surface plot of temperature distribution on tool insert at different surface positions.

Table 1. Experimental data

Parameters	Magnitude
Convective heat transfer coefficient, h	$10W/m^2K$
Thermal conductivity	$120W/m^2$
Initial temperature	$298K$
Density, ρ	$7800Kg/m^3$
Specific heat capacity, C_p	$343.3KJ/KgK$
Heat source, q_c	8.125×10^6W

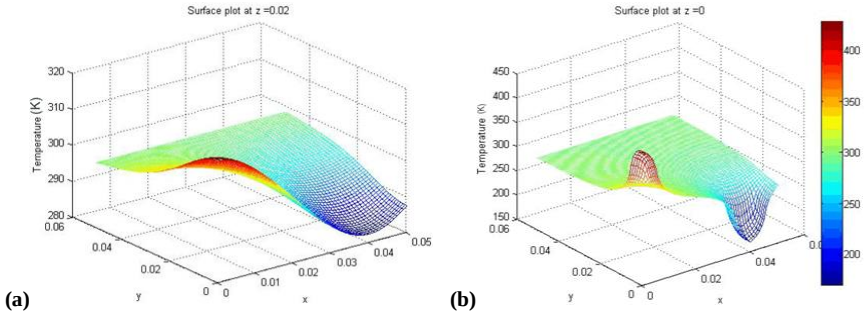

(a) (b)

Figure 2. (a) 3-D surface plot of temperature distributions on tool insert on surfaces (a) z = 0.02 and (b) z = 0.

Figure 2(a) shows the distribution of temperature at a surface $z=0.02$. It shows that the maximum temperature of 310 K occurs at the tool tip. Also, the temperature decreases across the tool insert to its extreme end which has a minimum temperature of 285 K. Figure 2(b) shows the temperature distribution at the bottom surface $z=0$. It is observed that the minimum and maximum temperatures of 200 and 400 K occur at extreme end and tip of the tool respectively.

Case 2: Contour plot of temperature distribution on tool insert at different surface positions.

Figure 3(a) and (b) show the temperature distribution at the bottom surface z = 0 and surface z = 0.02 respectively. It is evident that the minimum and maximum temperature regions occur at the extreme end and tip of the tool, respectively.

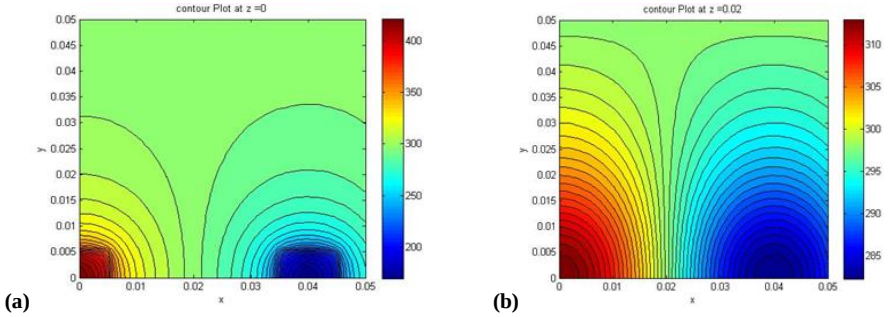

Figure 3. (a) Contour plot of temperature distributions on tool insert on surfaces (a) z = 0 and (b) z = 0.02.

Case 3: Profile plot of temperature distribution on tool insert at different surface positions.

Figures 4(a)-(d) show the temperature distribution on the surface z = 0 and x = 0, z = 0 and y = 0, z = 0.02 and x = 0, finally z = 0.02 and y = 0 respectively, whereby temperature decreases with distance from the machining zone. From the results obtained, it is evident that temperature varies with distance away from the tool tip, the machining zone. Figures 5(a) and (b) show the effect of velocity on temperature rise at the shear plane at different rake angles and cutting forces respectively, as Figure 6(a) shows the effect of cutting forces on temperature rise on shear plane at different rake angles. Figure 6(b) presents the effect of chip thickness ratio on temperature rise.

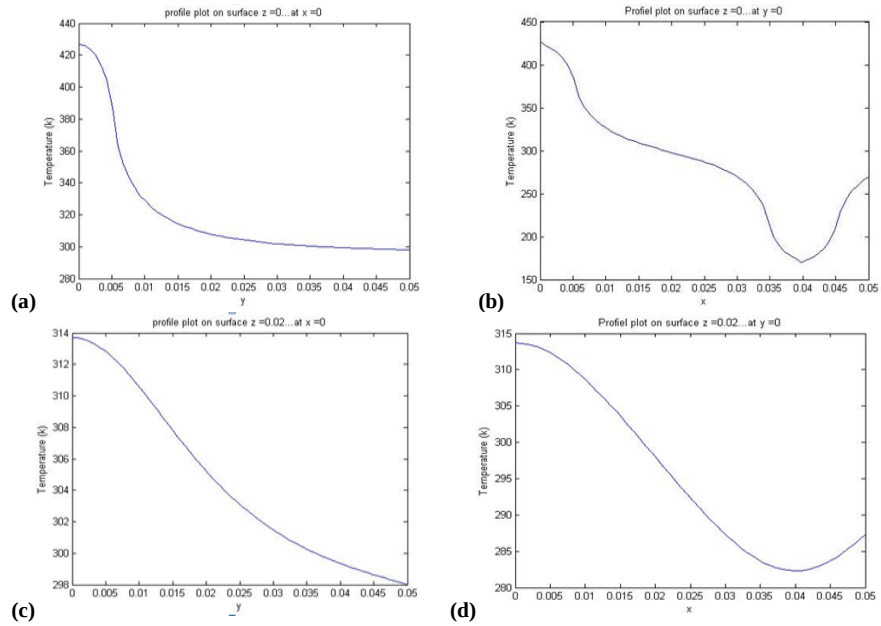

Figure 4. A 2-D profile plot of temperature distributions on tool insert on surfaces (a) z = 0 and point x = 0 (b) z = 0 and point y = 0, (c) z = 0.02 and x = 0, finally (d) z = 0.02 and y = 0.

Therefore, it can also be deduced that the thicker the chip thickness, the lower the temperature rise and the thinner the thickness, the higher the temperature rise. The increase of temperature can be attributed to the fact that friction as well as shearing at tool-chip interface has increased as un-deformed chip thickness becomes larger, thus, more heat is generated as un-deformed chip thickness increases.

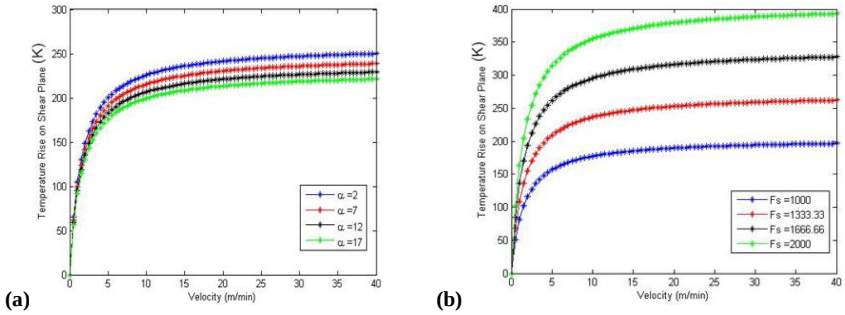

Figure 5. Temperature rise on shear plane against velocity at different (a) rake angles and (b) shear forces.

The Fourier law of heat conduction shows that the rate of heat loss is inversely proportional to the area of the surface in contact. Therefore, it can be concluded that temperature rises with reduction in thickness and falls with increment in thickness. This also validates the simulation results generated in this model. Furthermore, the effect of the chip thickness ratio on the maximum temperature at different rake angles is shown in Figure 6(c). It is observed that the thinner the thickness, the higher the maximum temperature at the shear plane. From the results, it is shown that at different rake angles, the effect of the chip thickness on the maximum temperature is the same, and the maximum temperature decreases with an increase in chip thickness ratio.

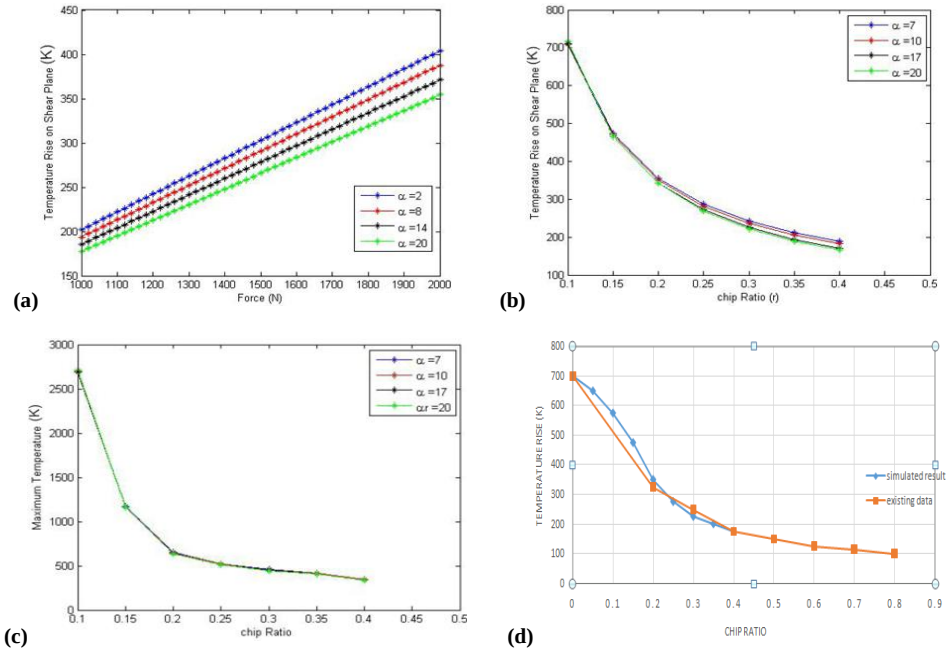

Figure 6. Temperature rise on shear plane against (a) force, (b) chip ratio, (c) maximum temperature against chip ratio, at different rake angles, and (d) model validation with extant experimental data.

Figure 6(d) shows the comparison of simulated model with existing data. It shows the temperature rise at the shear plane against the chip ratio. The existing data is gotten from Ojolo et al. [4], it is evident from Figure 6(d) that there is an increase in the temperature rise of the simulated results for chip ratios 0 – 0.25 mm, when compared with existing data. However, this temperature decreases between chip ratios 0.25 – 0.375 mm, as compared with the extant data. It can be concluded that the temperature rise decreases with increase in chip thickness ratio. Therefore, the simulation result is hereby validated, with close a close agreement in both results.

4. Conclusion

Temperature plays an important role in orthogonal machining in terms of thermal distortion of the tool and workpiece, and the dimensional accuracy of the machined parts as well as the tool life of the tool insert. In this work, the finite element analysis of the orthogonal machining was conducted, employing the method of separation of variables and MATLAB^{TM} finite element modelling software. This was developed to simulate the thermal behaviour of a carbide cutting tool in three dimensional dry machining. The temperature distribution depends on thermal conductivity, density, specific heat, shape and contact of the tool. Therefore, the FEM shows that the maximum temperature occurs at the tool tip and the temperature decreases with distance away from the tool tip. It also shows that the minimum temperature occurs at the extreme end of the tool insert.

References

[1] A.E. Diniz and D.R, Micaroni, D.R. (2002), 'Cutting conditions for finish turning process aiming the use of dry cutting', *International Journal of Machine Tools and Manufacture* **42** (1951), 889-904.

[2] H.Y.K. Portda and A.T. Zehnder, Measurements and simulations of temperature and deformation fields in transient metal cutting, *Journal of Manufacturing Science and Engineering* **125** (2003), 645-655.

[3] N.A. Abukhshim, P.T. Mativenga and M.A. Sheikh, Heat generation and temperature prediction in metal cutting: A review and implications for high speed machining, *International Journal of Machine Tools and Manufacture, Design, Research and Application* **46** (2006), 782-800.

[4] S.J. Ojolo, S.O. Ismail and O.T. Yusuf, Theoretical determination of temperature field in orthogonal machining, *International Journal of Engineering and Technology Innovation* **3** (2013), 240-253.

[5] A.E. Tay, M.G. Stevenson and D.G. Davis, Using the finite element method to determine temperature distribution in orthogonal machining, *Proceedings of the Institution of Mechanical Engineers* **188** (1974), 627–638.

[6] K.J. Trigger and B.T. Chao, An analytical evaluation of metal cutting temperature, *Transaction ASME Technical Paper* **73** (1951), 57–68.

[7] E.G Loewen, M.C. Shaw, On the analysis of cutting tool temperatures, *Transaction ASME Technical Paper* **76** (1954), 217–231.

[8] J.H. Weiner, Shear plane temperature distribution in orthogonal cutting, *Transaction ASME Technical Paper* **77** (1955), 1331–1341.

[9] P.K. Wright, M.C. McCormick and T.R. Miller, Effect of rake face design on cutting tool temperature distribution, *Journal of Engineering for Industries* **102** (1980), 123–128.

[10] P.K. Venuvinod and W.S. Lau, 'Estimation of rake temperatures in free oblique cutting', *International Journal of Machine Tools and Manufacture, Design, Research and Application* **26** (1986), 1–14.